GIS Application for Solar Potential Estimation on Buildings Roofs

Matej Brumen, Niko Lukač, Borut Žalik

University of Maribor,Faculty of Electrical Engineering and Computer Science,
Smetanova ulica 17, Maribor, Slovenia
emails: {matej.brumen@um.si, niko.lukac@um.si, borut.zalik@um.si}

***Abstract*—Over recent years, photovoltaic systems have become increasingly popular for the installation on buildings' rooftops. One of the main questions for investors is to find which rooftop is suitable for photovoltaic system installation in order produce maximum electrical energy. This paper presents Geographic Information System (GIS) for the solar and photovoltaic potential estimation for a whole municipality. The presented GIS consists of a server environment, web application, and mobile application. The developed application was successfully deployed within a regional project for the Municipality of Beltinci in Slovenia.**

Keywords-*GIS; Solar Potential Estimation; Web Application; Geoserver; LiDAR*

I. Introduction

Solar energy is a renewable energy source that can be converted into electrical energy using the photovoltaic (PV) effect. Since the advancement of PV technology buildings' rooftops have become suitable regions for generating electricity from the received solar irradiance (i.e., radiation incident on a surface). Of course, not all rooftops are appropriate for the installation of PV systems due to unsuitable topography and shadowing from the surrounding environment. Determination of a rooftop's suitability can be done using a manual survey by experts in this field. However, this process is highly unsuitable for the estimation of Solar Potential (SP) over a larger region with thousands of rooftops. An automated approach is necessary for larger regions. Such approaches produce results that are then displayed using web-based Geographics Information System (GIS) applications which allow users to overview SP estimation for their buildings' rooftops. There are many web applications that allow estimation of SP and each application displays results that are produced using a specific solar irradiance estimation method. Moreover, some applications allow the user to view the PV installation costs and the revenue over a few years regarding a given rooftop.

This paper presents a novel GIS for the SP estimation of rooftops. The system consists of a server and client applications. All data, including the calculated solar radiation data is stored on the server side of the environment. SP estimation is based on a newer method that considers analysing the meteorological data of solar irradiation and the simulation of shadowing over the classified Light Detection And Ranging (LiDAR) data using the method presented in [1] [2]. Furthermore, the shadowing from nearby vegetation and surrounding terrain is considered for SP evaluation. LiDAR is a remote sensing technology that emits laser impulses for determining the positions of objects on the landscape [3]. An unstructured 3D point-cloud of the landscape is obtained as a result of the scan. Therefore, the local topography can be estimated. The presented GIS is based on a newer SP estimation method, and provides more accurate insights into the suitable surfaces for PV systems' installation.

In the 2nd section, the methods for SP estimation and some web applications for viewing/calculating SP are presented. In the 3rd section, our method for SP estimation is presented together with the technologies used for server-side environment, web application and mobile application development. In the 4th section, the results of our methods and applications are shown and are concluded in the 5th section.

II. Related Work

A. Solar Potential Estimation

The use of geospatial data for automatic solar potential estimation is the first step towards accurate solar potential estimations for buildings' rooftops within urban areas. Several different models have been suggested [4]–[9] that use topographical characteristics of the Digital Elevation Model (DEM). Ruiz-Arias et al. [10] conducted a detailed comparison of the better-known models for the solar potential estimation, and reported the r.sun model [9] as being one of the most accurate. Voegtle et al. [11] analysed the solar potential on rooftops in urban areas. Kassner et al. [12] represented LiDAR as 2.5D point-cloud in order to estimate solar potential with the help of masked roof contours. Jochem et al. [13] introduced the method for automatic roofs' planes detection in the 3D point cloud by using an implementation for solar potential estimation based on [9]. Their method uses the clear-sky index (CSI). Hofierka and Kanuk [14] also used the r.sun model for solar potential estimation within urban areas. Jochem et al. [15] introduced transparent shadowing caused by vegetation when calculating the solar potential. They considered the ratio between the first and the last echos of the laser pulses for the measurement of transparency. Such vegetation shadowing can only be used during the specific season when the scanning was performed. A more accurate approach was used by Levison et al. [16] with the use of high resolution ortophotos and LiDAR, together with the vegetation growth model, in order to predict the impact of rooftop shading and solar irradiance. The authors had manually surveyed and classified the data for accurate

 ISBN: 978-1-61208-333-9

simulation of the vegetation growth. Hence, only smaller urban areas could be analysed in reasonable time.

B. GIS Applications For Solar Potential

There are many web-based environments that allow the user to overview the irradiance or PV estimation of the rooftops over a local region. Comparisons between different features of these applications are shown in Table [I]. The considered features are:

- Cell colouring: if the application provides an additional layer, where the cells are coloured with the intensity of solar radiation by using a colouring scale.
- Monthly PV details: if the application considers further information about the monthly solar potential values for the selected building.
- Investment plan: if the application provides any investment plans for the users that want to install solar panels on their rooftops.
- Rooftop details and ROI: if the application provide additional information about the selected rooftop or its selected part via user-selectable Region Of Interest (ROI). Some application partially support this by providing only one of these two features.
- User parameters: if an application supports entry fields for user specified parameters (rooftop angle and orientation, rooftop usability percentage).
- Rooftop angle consideration: if the application considers rooftop angles during the solar potential estimation. This could be obtained from custom user parameters or extracted from LiDAR point cloud.

Some applications provide further analysis, such as economical investment planning over the selected rooftops, whilst other types of applications display coloured cells as a new raster/vector layer over the rooftops or the entire region. Few display the measured data of the existing PV systems installed on rooftops.

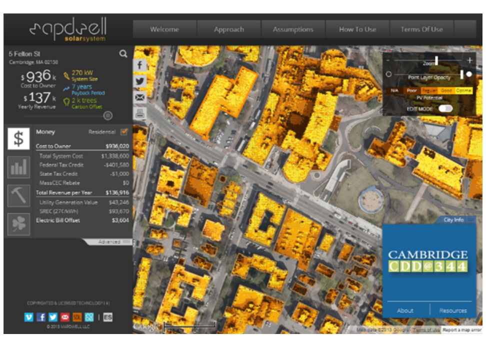

Figure 1. Overview of the solar potential vector layer over the rooftops using the Mapdwell solar tool [27].

There are different types of data representation in GIS-based applications. The two more advanced applications from Table I were considered for a more detailed comparison. These applications were Mapdwell Solar Tool [27] [28] and NYC Solar Map [23]. Both applications support solar potential estimation for selected parts of the rooftop and the calculation for a detailed investment plan. The main difference is that Mapdwell Solar Tool has a visual representation using a vector layer (i.e., pixels coloured by intensity) of the solar potential values (see Figure 1). This feature has an visual advantage for quickly finding which parts of the rooftops are the most suitable. However, this is more difficult to achieve on NYC Solar Map because the user has to first select each rooftop to acquire detailed information of the solar potential estimation, whilst not having a more detailed visual overview as to which parts are more suitable (see Figure 2).

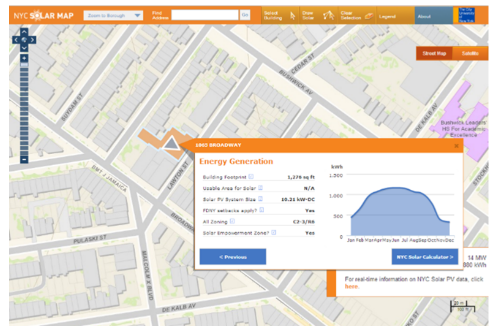

Figure 2. Detailed overview of the solar potential for the selected rooftop area on the NYC Solar Map [23].

The presented GIS application supports both the solar potential raster layer and the detailed per-building description, and is explained in more detail within the next sections.

III. SOLAR POTENTIAL ESTIMATION AND GIS ENVIRONMENT

The first subsection briefly summarises the theoretical background of the used solar potential method, whilst the following three subsections present the developed GIS application that consists of server, web, and mobile environments. The entire workflow of the presented GIS, reflecting the considered design choices, can be seen in Figure 3.

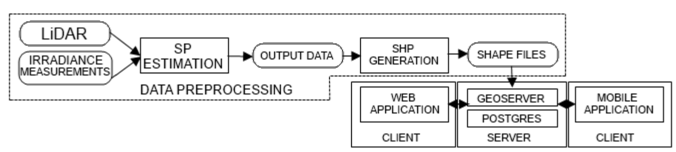

Figure 3. Workflow of the proposed GIS, where normal rectangles represent services and applications, while rounded rectangles represent the data.

A. Solar Potential Estimation

Solar potential is estimated using a newer method [1], where multiresolutional shadowing is considered as well long-term irradiance measurements by a pyranometer. Heuristic variable shadowing from vegetation is also considered in the estimation.

At first the LiDAR data is arranged into a regular grid consisting of 2.5D cells. The size of each cell is set at $1m^2$. The height of the cell is defined by the highest point of the points

 ISBN: 978-1-61208-333-9

TABLE I. COMPARISON OF DIFFERENT GIS APPLICATIONS FOR THE SOLAR POTENTIAL ESTIMATION.

Application/Feature	Cell colouring	Monthly PV details	Investment plan	Rooftop details and ROI	User parameters	Rooftop angle consideration
Anaheim [17]	YES	NO	NO	NO	NO	NO
Berkley [18]	NO	N/A	N/A	NO	NO	N/A
Boston [19]	YES	YES	YES	YES	YES	NO
Denver [20]	NO	YES	NO	NO	NO	NO
Los Angeles [21]	YES	NO	NO	Partial	NO	NO
Madison [22]	YES	YES	YES	Partial	YES	YES
NYC [23]	NO	YES	YES	YES	NO	YES
Salt Lake City [24]	YES	YES	NO	Partial	YES	YES
San Diego [25]	YES	NO	NO	Partial	NO	YES
San Francisco [26]	NO	NO	NO	Partial	NO	NO
Mapdwell (Cambridge) [27] [28]	YES	NO	YES	YES	NO	YES
Dachflächeneignung für Solaranlagen [29]	Partial	NO	NO	Partial	NO	N/A
Bristol [30]	Partial	NO	NO	Partial	NO	N/A
Wien [31]	YES	NO	NO	Partial	NO	N/A

within a cell. The daily solar irradiance is then calculated as:

$$I(t) = \int_{se}^{sw} (I_b(t)(1 - S(t)) + I_d(t))[Wm^{-2}], \qquad (1)$$

where t is the calculation time-step, *se* and *sw* are sunrise and sunset, I_b the calculated direct radiation, I_d the calculated diffuse radiation and $S(t) \in [0, 1]$ the shadowing factor. Time and space-dependent shadowing depends on an accurate positioning of the Sun, which can be obtained with the Almanac algorithm [32]. The per-cell irradiance is calculated by considering many topographical relationships, such as slope and orientation. The solar potential is then computed as cumulative yearly irradiance in Watt hours per square meter $[Whm^{-2}]$:

$$P(t) = \sum_{t=1}^{365} I(t)[Whm^{-2}]. \qquad (2)$$

Additionally, $P(t)$ can be multiplied by the constant efficiency factor for a given semi-conducting material in order to estimate approximate electrical energy production. The constant efficiency is usually taken as the peak-efficiency of a given semiconducting material depending on the type of PV module. Recently, newer methods [33] [34] are being developed for more accurate PV potential estimation.

Once the calculation is complete, the output data is converted into the Environmental Systems Research Institute (ESRI) shape file, where each cell location is stored together with the values of the estimated solar potential.

B. Server Side Of The Environment

Geographical information systems are available as standalone desktop applications (Quantum GIS [35], The Integrated Land and Water Information System (ILWIS) [36]) or network services (GeoServer [37], Mapnik [38]) running on remote computers. Server applications support Web Map Service (WMS) and Web Feature Service (WFS) requests, where results are returned as WFS or WMS layers to the client-side applications that process the requested data.

The GeoServer and PostgreSQL applications are used on the server-side. GeoServer [37] is an open-source server solution written in Java. The GeoServer allows the management of the WFS and WMS requests that are specified by Open Geospatial Consortium (OGC) [39]. Geospatial data is stored in the PostgreSQL [40] database with a PostGIS [41] extension. Data from SP estimation are converted into an ESRI Shape format (SHP) and imported into the database that can be accessed from the GeoServer. A proper colouring technique is required because no colour value is stored in the solar shape file. The GeoServer provides the OGC standardised Styled Layer Descriptor language (SLD) that is used for customising the shape colors according to the specified attribute values. Colouring of the shapes is divided into 6 groups.

Each group has its own colour, e.g., groups $group_0$ to $group_5$ are coloured in black, blue, cyan, green, yellow, and red. The initial value of $group_0$ is $min(solarpotential)$ and the value of $group_5$ is $max(solarpotential)$. The rest of the key values are calculated as:

$$v_i = (P_{max} - P_{min}) \cdot 0.2 + v_{i-1}. \qquad (3)$$

The remaining values are interpolated.

C. Web Application

A web-based client application is necessary in order to visualise the stored data and the pre-calculated solar potential. Therefore, a good solution is to create a web-based client application that consists of a map view for showing ortophotos and the solar potential raster layer of the rooftops within a local region. The simple point-in-polygon test can be performed by using the combined data of the estate vector maps together with their address information. The solar map is then aligned to the vector map, as shown in Figure 4.

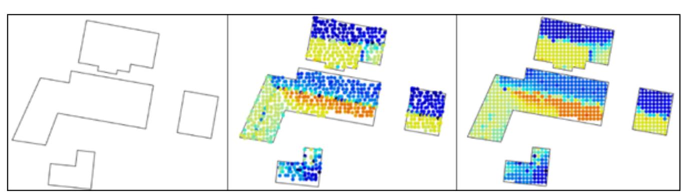

Figure 4. Alignment of the cells (left: building shape; middle: disarranged cells; right: arranged cells).

When using this method, all the solar cells can be linked to the rooftops and simple requests for each rooftop can be made. Hence, the users can select the rooftops to see detailed

 ISBN: 978-1-61208-333-9

graphs of the cumulative calculated solar irradiance throughout the year. OpenLayers [42] is used for displaying the necessary layers via WMS. The WFS requests are used for obtaining geometry and attribute data. The result of these requests is the output formatted with Geometry Markup Language (GML), which can be parsed with OpenLayers API. The JQuery [43] libraries are used for Graphical User Interface (GUI) with which simple pop-up windows can be created for displaying details. Moreover, a Portable Document Format (PDF) report can be obtained for the detailed information of a given rooftop. PDF reports were generated by using LaTeX interpreter.

D. Mobile Application

Mobile devices are increasing in performance and supporting many hardware and software features. Therefore, a mobile application can provide the same amount of information as the web-based application, whilst it also supports the nearest object search with the use of Global Positioning System (GPS) technology. The developed application is supported on devices with Android 2.2 or a higher version. The tabbed view is used to categorise information about the calculated solar potential because many of the devices still have low-resolution displays. The map is shown on the first tab, where the users can navigate through the area and look for suitable roofs. With the simple selection of the rooftop, the detailed data about that rooftop can be viewed within the second tab. On the map tab the ”WebView” component is used where the mobile version of the presented web-application is loaded, which is a simplified version targetted for mobile devices. Using the Javascript interfaces that are enabled on Android, the Java and Javascript code can be connected together. For example, methods implemented in Java (Android Application) can be accessed from Javascript file on the web. This technique is used for the data transfer when the user taps on the rooftop. Application supports the GPS search of the nearest roof, and also considers the devices' orientations. Then it transmits the GPS coordinates and orientation values to the server in order to find the closest rooftop. When the search is completed on the server, the ID of the building is transferred back to the mobile application, and the building with received ID is selected.

IV. Results

Solar potential estimation and GIS-based application were successfully applied for the Municipality of Beltinci in Slovenia, where the estimation was performed over 5605 rooftops. The deployed web application is accessible at [44]. The mobile application can be obtained at Google Play under the name SolarEnergo, which currently only supports the Slovene language. The total solar potential for all the considered rooftops was estimated at 181 GWh per year, and the PV potential was within a range from 16 GWh to 26 GWh, depending on the type of PV material. The first step was to obtain the classified LiDAR data (see Figure 5), and to estimate the solar potential for each rooftop. The considered solar potential estimation method also required the use of long-term diffuse and direct irradiance data from the nearby meteorological station.

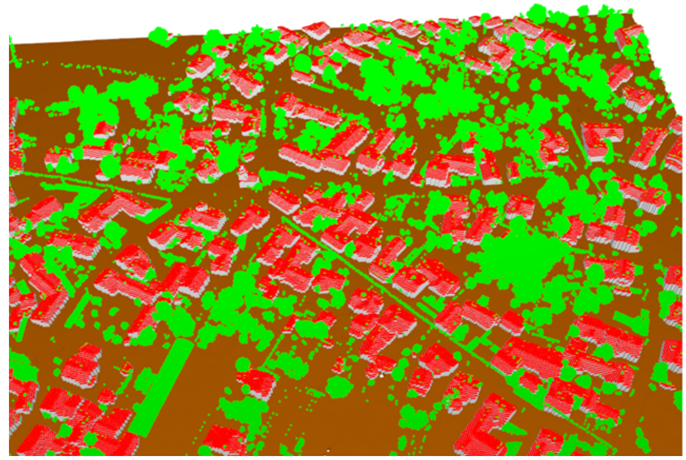

Figure 5. Visualisation of the regular grid created from point cloud of LiDAR, which is classified data into buildings, vegetation, and terrain.

The solar potential was estimated over a regular grid that was created from LiDAR point-cloud. The grid consists of multiple cells where each cell contains position, solar potential, and approximate PV potential based on constant efficiency characteristics for amorphous and polycrystalline cells. In the second step each cell's information was prepared and converted into a GeoServer supported format. The output was converted into multiple shape files (see Figure 6) from which the PDF reports were generated. All of the data was then inserted into the database that can be accessed from the developed applications via GeoServer. The colour of each cell was based on its solar potential value, where the style was defined by GeoServer.

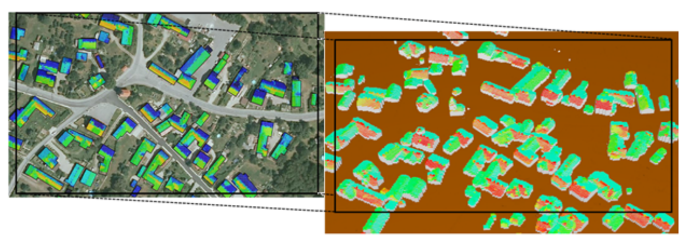

Figure 6. Graphical overview of the solar potential values for the same region of the WMS layer on GeoServer (left) and the regular grid of the LiDAR data (right).

When a user selects a given rooftop, the detailed data is shown in the pop-up window. These data consists of a building's address, the total solar potential throughout the year, and the approximately produced electricity. There is an additional graph where the data for each month are displayed (see Figure 7). SP and PV values in the graph are represented by different colors. The brown colour represents PV potential for A-Si material, red is for P-Si material and blue colour represents the solar potential.

HTML5 supported browser is necessary for this functionality. Detailed PDF reports are also available for each building's rooftop. The user can input an address in order to locate a given building whilst also receiving suggestions of similar addresses from the server. Moreover, the shadowing caused by vegetation and other buildings can be seen in Figure 7. The

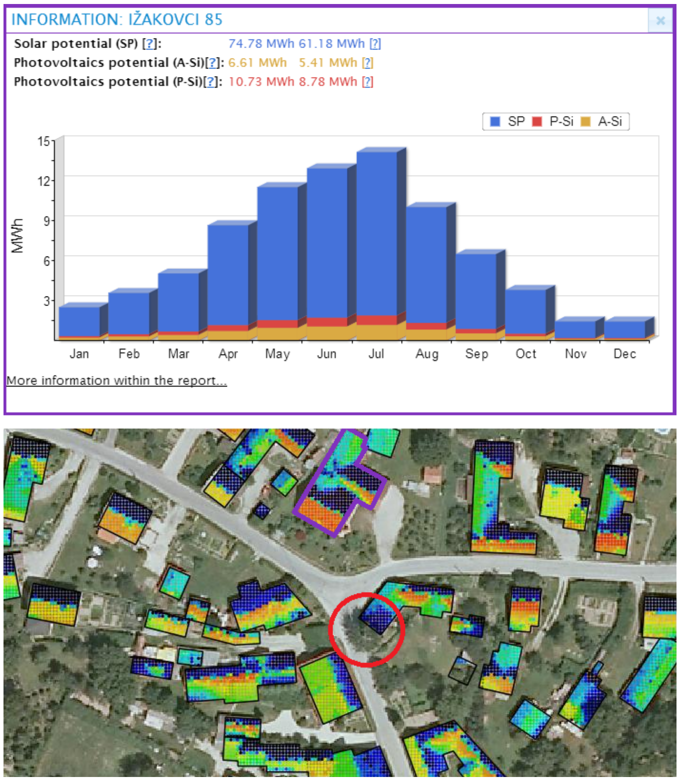

Figure 7. Detailed overview of the calculated solar potential for the selected building. The marked area in the red circle represents an example of reduced solar potential due to shadowing from high-vegetation.

deciduous type of vegetation is less dense during the winter, and has lower impact on the rooftop' shadowing. In Figure 8, the Android application is shown that is a light version of the web-application.

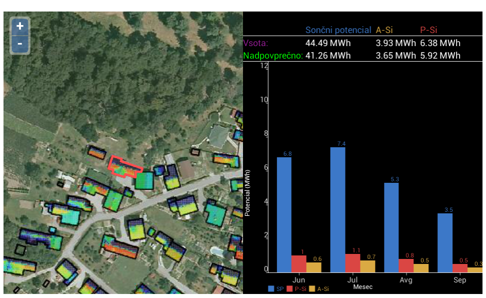

Figure 8. Screenshot of the mobile application, where the used language is Slovene. Two views are shown, namely the map view (left) and the details view (right), where the graph of the monthly estimations is displayed.

There are no significant bottlenecks on the server side, since all the calculations are preprocessed beforehand. The only possible time consuming operation is the generation of the raster tiles that consist of multiple layers in the database. These layers represent different data types: orthophoto, buildings shape layer and SP layer. Furthermore, the rasterization operation of the geometry from SP layer is also one of the heavier task for Geoserver. Due to possible server overload, the users can notice slower loading times for tiles (especially those with SP cells) in their client applications.

Additional statistics were made from the SP data. Detailed overview on how the rooftops' cells slope and aspect values affects the received SP (see Figure 9). Total amount of grid cells was 978282.

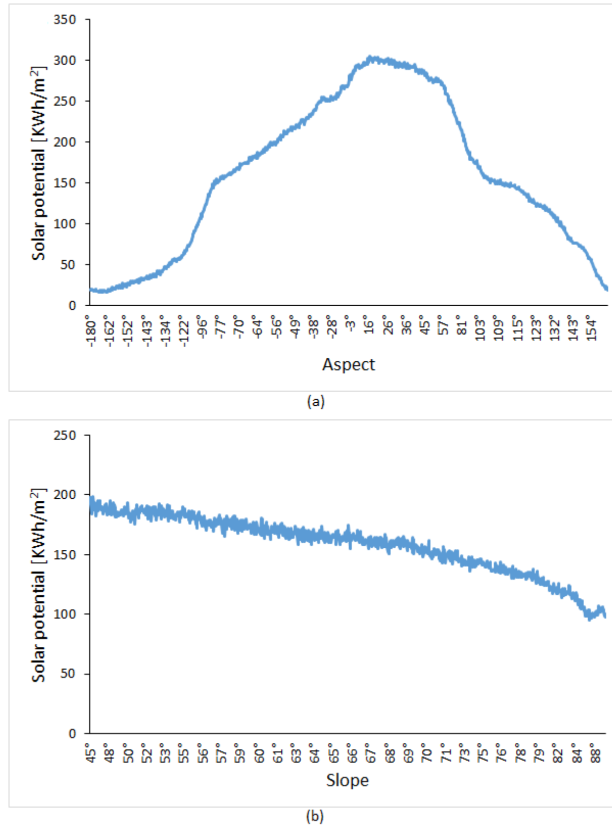

Figure 9. Graph of SP values through different cell (a) aspects and (b) slopes.

Figure 9.a represents the rooftop cell aspect (cell orientation), where the highest SP was observed at surfaces oriented towards the geographic south (i.e., 0 aspect). On the second graph (see 9.b), information on how the cell slope can affect on the received SP. Cells with slope perpendicular to average direction of the Sun's radiation (i.e., near 45) can receive higher irradiance than cells with other slopes.

V. Conclusion

In this paper, the development of a GIS application was described that allows users to quickly locate suitable rooftop areas with the help of the calculated solar potential. This application provides deep insight into estimated monthly received solar irradiance, as well as approximate prediction of the produced electrical energy. Therefore, such type of applications help improve sustainability of modern cities. Furthermore, the presented application uses a recent method for the solar potential estimation, where long-term diffuse and direct irradiance measurements were considered, as well as shadowing from vegetation and surrounding terrain. Additionally, a mobile application was developed, where the user can select the nearest rooftop by using the GPS technology. From the implementation perspective, it is important to preprocess as much of calculations as possible, in order to decrease the computing load on the web servers. Additionally, the accuracy

 ISBN: 978-1-61208-333-9

highly depends on the input data (i.e., resolution of LiDAR point cloud and long term irradiance measurements), therefore when creating similar applications in the future, modern classification methods for LiDAR data should be considered, and an accurate solar irradiance model.

VI. Acknowledgements

Thanks to the Surveying and Mapping Authority of the Republic of Slovenia and Slovenian Environment Agency for providing the estate and irradiance data. Additionally, we would like to thank the Municipality of Beltinci that was coordinating the regional project DoFPoLO, which was supported by the Ministry of Education, Science, and Sport, as well the European Regional Development Fund. This research was supported by grants J2-5479 and P2-0041.

References

[1] N. Lukač, D. Žlaus, S. Seme, B. Žalik, and G. Štumberger, "Rating of roofs surfaces regarding their solar potential and suitability for PV systems, based on LiDAR data," Applied Energy, vol. 102, 2012, pp. 803 – 812.

[2] N. Lukač and B. Žalik, "GPU-based roofs' solar potential estimation using LiDAR data," Computers & Geosciences, vol. 52, 2013, pp. 34 – 41.

[3] G. Petrie and C. Toth, "Airborne and spaceborne laser profilers and scanners," In: Shan J, Toth CK, editors. Airborne and spaceborne laser profilers and scanners. Boca Raton: CRC Press, vol. 54, 2008, pp. 29–86.

[4] W. Hetrick, P. Rich, F. Barnes, and S. Weiss, "GIS-based solar radiation flux models." American Soc Photogrammetry & Remote Ssnsing+ Amer Ccong ON., vol. 3, 1993, p. 132.

[5] R. Dubayah and P. Rich, "Topographic solar radiation models for GIS," International Journal of Geographical Information Systems, vol. 9(4), 1995, pp. 405–419.

[6] L. Kumar, A. Skidmore, and E. Knowles, "Modelling topographic variation in solar radiation in a GIS environment," International Journal of Geographical Information Science, vol. 11(5), 1997, pp. 475–497.

[7] P. Fu and P. M. Rich., "A geometric solar radiation model with applications in agriculture and forestry," Computers and electronics in agriculture, vol. 37(1), 2002, pp. 25–35.

[8] J. G. Corripio, "Vectorial algebra algorithms for calculating terrain parameters from dems and solar radiation modelling in mountainous terrain," International Journal of Geographical Information Science, vol. 17(1), 2003, pp. 1–23.

[9] M. Šúri and J. Hofierka, "A new GIS-based solar radiation model and its application to photovoltaic assessments," Transactions in GIS, vol. 8, 2004, pp. 175–190.

[10] J. Ruiz-Arias, J. Tovar-Pescador, D. Pozo-Vázquez, and H. Alsamamra, "A comparative analysis of DEM-based models to estimate the solar radiation in mountainous terrain," International Journal of Geographical Information Science, vol. 23(8), 2009, pp. 1049–1076.

[11] T. Voegtle, E. Steinle, and D. Tovari, "Airborne Laser scanning data for determination of suitable areas for photovoltaics," Remote Sensing and Spatial Information Sciences, vol. 36(3/W19), 2005, pp. 215–220.

[12] R. Kassner, W. Koppe, T. Schüttenberg, and G. Bareth, "Analysis of the solar potential of roofs by using official LiDAR data," In Proceedings of the International Society for Photogrammetry, Remote Sensing and Spatial Information Sciences, (ISPRS Congress), 2008, pp. 399–404.

[13] B. Jochem, Höfle, M. Hollaus, and M. Rutzinger, "Object detection in airborne LiDAR data for improved solar radiation modeling in urban areas," Remote Sensing and Spatial Information Sciences, vol. 38(part 3), 2009, p. W8.

[14] J. Hofierka and J. Kaňuk., "Assessment of photovoltaic potential in urban areas using open-source solar radiation tools," Renewable Energy, vol. 34(10), 2009, pp. 2206–2214.

[15] A. Jochem, H. Bernhard, and R. Martin, "Extraction of vertical walls from mobile laser scanning data for solar potential assessment," Remote Sensing, vol. 3(4), 2011, pp. 650–667.

[16] R. Levinson, H. Akbari, M. Pomerantz, and S. Gupta, "Solar access of residential rooftops in four California cities," Solar Energy, vol. 83(12), 2009, pp. 2120–2135.

[17] City of Anaheim Solar Map Template. [retrieved: 10, 2013]. [Online]. Available: http://anaheim.solarmap.org/

[18] Berkley Solar Map. [retrieved: 10, 2013]. [Online]. Available: http://berkeley.solarmap.org/

[19] Boston Solar. [retrieved: 10, 2013]. [Online]. Available: http://gis.cityofboston.gov/SolarBoston

[20] DRCOG Denver Regional Solar Map. [retrieved: 10, 2013]. [Online]. Available: http://solarmap.drcog.org/

[21] LA Country Solar Tool and Green Planning Tool. [retrieved: 10, 2013]. [Online]. Available: http://solarmap.lacounty.gov/

[22] City of Madison. Wis MadiSUN. [retrieved: 10, 2013]. [Online]. Available: http://solarmap.cityofmadison.com/madisun/

[23] NYC Solar Map. [retrieved: 10, 2013]. [Online]. Available: http://nycsolarmap.com/

[24] Salt Lake City Solar. [retrieved: 10, 2013]. [Online]. Available: http://www.slcgovsolar.com/

[25] San Diego Solar. [retrieved: 10, 2013]. [Online]. Available: http://sd.solarmap.org/solar/index.php

[26] San Francisco Solar Map. [retrieved: 10, 2013]. [Online]. Available: http://sf.solarmap.org/

[27] Mapdwell Solar System. [retrieved: 10, 2013]. [Online]. Available: http://www.cambridgema.gov/solar/

[28] R. C. F. Jakubiec, J. A., "Towards validated urban photovoltaic potential and solar radiation maps based on lidar measurements, GIS data, and hourly daysim simulations," in 5th National Conference of IBPSA-USA, Madison, Wisconsin., 2012.

[29] Dachflächeneignung für Solaranlagen. [retrieved: 12, 2013]. [Online]. Available: http://geo.gkd-el.de/website/solar/viewer.htm

[30] Bristol. [retrieved: 12, 2013]. [Online]. Available: http://maps.bristol.gov.uk/pinpoint/?service=localinfo&maptype=js&layer=Neighbouring+authorities;Solar+potential

[31] Wien Umweltgut. [retrieved: 11, 2013]. [Online]. Available: http://www.wien.gv.at/umweltgut/public/grafik.aspx?ThemePage=9

[32] J. J. Michalsky, "The Astronomical Almanac's algorithm for approximate solar position." Solar Energy, vol. 40.3, 1988, pp. 227–235.

[33] R. C. F. Jakubiec, J. A., "A method for predicting city-wide electricity gains from photovoltaic panels based on LiDAR and GIS data combined with hourly Daysim simulations," Solar Energy, vol. 93, 2013, pp. 127–143.

[34] N. Lukač, S. Seme, D. Žlaus, G. Štumberger, and B. Žalik, "Buildings roofs photovoltaic potential assessment based on LiDAR (Light Detection And Ranging) data," Energy, vol. In Press, 2014.

[35] Quantum GIS. [retrieved: 10, 2013]. [Online]. Available: http://www.qgis.org/en/site/

[36] ILWIS. [retrieved: 10, 2013]. [Online]. Available: http://www.ilwis.org/

[37] GeoServer. [retrieved: 09, 2013]. [Online]. Available: http://geoserver.org/display/GEOS/Welcome

[38] Mapnik. [retrieved: 09, 2013]. [Online]. Available: http://mapnik.org/

[39] Open Geospatial Consortion. [retrieved: 10, 2013]. [Online]. Available: http://www.opengeospatial.org/standards

[40] PostgreSQL Database. [retrieved: 10, 2013]. [Online]. Available: http://www.postgresql.org/

[41] PostGIS - Spatial and Geographic objects for PostgreSQL. [retrieved: 10, 2013]. [Online]. Available: http://postgis.net/

[42] OpenLayers. [retrieved: 10, 2013]. [Online]. Available: http://openlayers.org

[43] JQuery. [retrieved: 11.2013]. [Online]. Available: http://jquery.com/

[44] SolarEnergo. [retrieved: 03, 2014]. [Online]. Available: http://solarenergo.beltinci.si/en/